ISSN: 3079-9341

Formate-Dominated Reaction Networks on ZrO2-Modified Cu Surfaces

Jean-Pierre Dubois[1], Camille Laurent[2], François Martin[3]*

Laboratoire de Réactivité de Surface, Sorbonne Université, 4 Place Jussieu, 75005 Paris, France

***Corresponding author:** francois.martin@sorbonne-universite.fr

Abstract

Reaction pathway selection critically determines product distribution in CO2 hydrogenation. In this study, a comprehensive reaction network consisting of 41 elementary steps was constructed using density functional theory to compare formate- and CO-mediated pathways on ZrO2-decorated Cu surfaces. Energetic span analysis shows that ZrO2 modification reduces the energetic span of the formate route from 1.05 eV on Cu to 0.69 eV at the interface, while simultaneously increasing the barrier for CO formation. Microkinetic simulations predict methanol selectivities exceeding 75% across a temperature range of 500–540 K, in contrast to CO-dominated behavior on Cu. The analysis identifies hydrogenation of bidentate formate as the primary rate-determining step under industrially relevant pressures. These results clarify how inverse catalysts fundamentally reshape the reaction network to favor methanol formation.

Keywords

formate pathway; reaction network; energetic span; ZrO2/Cu; CO2 hydrogenation

1.Introduction

The catalytic hydrogenation of carbon dioxide (CO_2) to methanol has attracted sustained interest as a promising route for carbon recycling and low-carbon fuel production [1]. Methanol serves not only as a versatile chemical feedstock but also as an energy carrier compatible with existing infrastructure, making this reaction highly relevant for both environmental mitigation and industrial application [2]. However, conventional Cu-based catalysts employed in industrial processes typically suffer from limited CO_2 conversion efficiency and suboptimal methanol selectivity, particularly under conditions favoring thermodynamic equilibrium [3]. These limitations have motivated the exploration of alternative catalyst architectures that can more effectively regulate surface reaction pathways. Among the strategies proposed, inverse catalyst systems—where oxide nanoparticles are dispersed on a metallic substrate—have emerged as a particularly effective design concept [4]. In contrast to traditional supported metal catalysts, inverse configurations enable the formation of extended oxide–metal interfacial regions that exhibit distinct electronic and

ISSN: 3079-9341

geometric characteristics [5]. The ZrO_2-on-Cu inverse catalyst has been shown to combine high structural stability with enhanced catalytic activity toward CO_2 hydrogenation. Recent work has demonstrated that such systems do not rely on a single uniform active site but instead operate through an ensemble of interfacial sites with differentiated catalytic roles, which collectively promote methanol formation over competing products [6]. This insight highlights the critical importance of explicitly resolving interfacial chemistry when analyzing reaction mechanisms on inverse catalysts. Despite growing experimental and theoretical interest, the mechanistic understanding of CO_2 hydrogenation on oxide–metal interfaces remains incomplete. Two dominant reaction routes are commonly proposed: the formate pathway, involving hydrogenation of surface formate species, and the reverse water–gas shift (RWGS)–derived CO pathway, which proceeds through CO intermediates prior to methanol formation [7]. Discriminating between these pathways is essential for rational catalyst design, as they lead to markedly different selectivity outcomes. Interfacial sites have been suggested to stabilize oxygenated intermediates, thereby shifting reaction flux toward methanol rather than CO formation [8]. However, many existing mechanistic studies rely on simplified surface models and limited reaction sequences, which restrict their predictive capability. A key limitation in current density functional theory (DFT)–based investigations is the use of truncated reaction networks. Most reported studies examine fewer than 10–15 elementary steps and primarily focus on the most direct hydrogenation routes, often neglecting side reactions, competitive adsorption processes, and alternative intermediate transformations [9]. This simplification can introduce substantial uncertainty in predicted energetics and product distributions [10]. In addition, kinetic analyses frequently adopt fixed apparent activation barriers, without explicitly accounting for the energetic span of the full catalytic cycle. Energetic span theory provides a more rigorous framework for linking thermodynamic landscapes to turnover frequencies, yet it remains underutilized in CO_2 hydrogenation modeling [11]. As a result, existing models struggle to reconcile theoretical predictions with the high methanol selectivity observed experimentally on ZrO_2-on-Cu inverse catalysts. To address these gaps, comprehensive reaction networks that integrate detailed energetics with microkinetic modeling are required [12]. Such approaches allow competing pathways to be evaluated on a consistent basis and enable identification of the true rate-determining states governing catalytic performance [13]. In particular, resolving how interfacial ensembles modulate reaction energetics across extended networks is crucial for understanding why inverse catalysts outperform conventional systems. In this work, a detailed reaction network comprising 41 elementary steps is constructed for CO_2 hydrogenation on a ZrO_2-on-Cu

ISSN: 3079-9341

inverse catalyst surface. Both the formate-mediated and CO-mediated pathways are systematically analyzed using energetic span theory to quantify their intrinsic kinetic favorability. Microkinetic simulations are employed to predict methanol selectivity across a range of temperatures and reaction conditions. By explicitly identifying the turnover-determining transition state and intermediate, this study clarifies how oxide–metal interfacial ensembles reshape the reaction landscape to favor methanol formation. The results provide mechanistic insight that bridges prior experimental observations and theoretical predictions, offering guidance for the rational design of next-generation inverse catalysts for CO_2 conversion.

2. Materials and Methods

2.1 Description of Computational Models

A periodic slab model represented the catalyst surface. A four-layer Cu(111) slab was used as the base. A Zr_3O_6 cluster was placed on the top layer to form the interface. The bottom two layers were fixed to model the bulk material. A vacuum space of 15 Å separated the layers. The system contained 85 atoms. This size balances accuracy and cost.

2.2 Experimental Design and Controls

The study compared two systems. The experimental group used the ZrO_2-modified Cu surface. The control group used the clean Cu(111) surface. This comparison shows the effect of the interface. The network included 41 steps. These steps covered the formate and CO pathways. This list ensures no path is missed.

2.3 Measurement and Quality Control

DFT calculations used the VASP code. The PBE functional described the energy. The PAW method treated the ion-electron interactions. A cutoff energy of 400 eV was used. The structure was relaxed until forces on free atoms were below 0.02 eV/Å. The CI-NEB method found the transition states. Frequency analysis confirmed one imaginary mode for each transition state.

2.4 Data Processing and Formulas

The Energetic Span Model assessed the efficiency. The energetic span (δE) controls the turnover frequency. It is calculated by Eq. (1):

$$\delta E=\max(T_{TS}-I_{int}+\Delta G_r)$$

ISSN: 3079-9341

Here, T_{TS} is the transition state energy, and I_{int} is the intermediate energy. The reaction rate (r) uses the law of mass action, as shown in Eq. (2):

$$r=k\prod_{i}\theta_i^{\nu_i}$$

Here, k is the rate constant, θ_i is the coverage, and ν_i is the coefficient.

2.5 Statistical Analysis and Conditions

Microkinetic simulations calculated the steady-state coverage. The LSODA algorithm solved the equations. The temperature ranged from 500 K to 600 K. The pressure was 50 bar. The H_2/CO_2 ratio was 3:1. Gibbs free energy corrections included zero-point energy, enthalpy, and entropy. These values came from the vibrational frequencies.

3.Results and Discussion

3.1 Analysis of the Reaction Network

A reaction network with 41 elementary steps was constructed to map the conversion of CO_2. The network covers two competing routes: the formate (HCOO*) pathway and the reverse water-gas shift (RWGS) pathway via carboxyl (COOH*) species. DFT calculations show that CO_2 adsorption at the ZrO_2–Cu interface releases 0.45 eV. This binding energy is stronger than on pure copper. The calculations confirm that the formate pathway is the main route. The formation of the bidentate formate species (b-HCOO*) acts as a stable intermediate. This stability prevents the desorption of unreacted CO_2 and pushes the reaction forward [14].

3.2 Energetic Span and Rate-Determining Steps

The Energetic Span Model was used to evaluate the cycle efficiency. This method identifies the states that control the turnover frequency. On the ZrO_2-modified surface, the energetic span is 0.69 eV. This value is lower than the 1.05 eV span on pure Cu(111). Fig. 1 shows the potential energy profile for the most favorable pathway. As shown in the figure, the rate-determining step is the hydrogenation of the bidentate formate to dioxomethylene (H_2COO*). The interface lowers the barrier for this step by stabilizing the oxygen-bound transition state [15]. This stabilization is not possible on a flat metal surface.

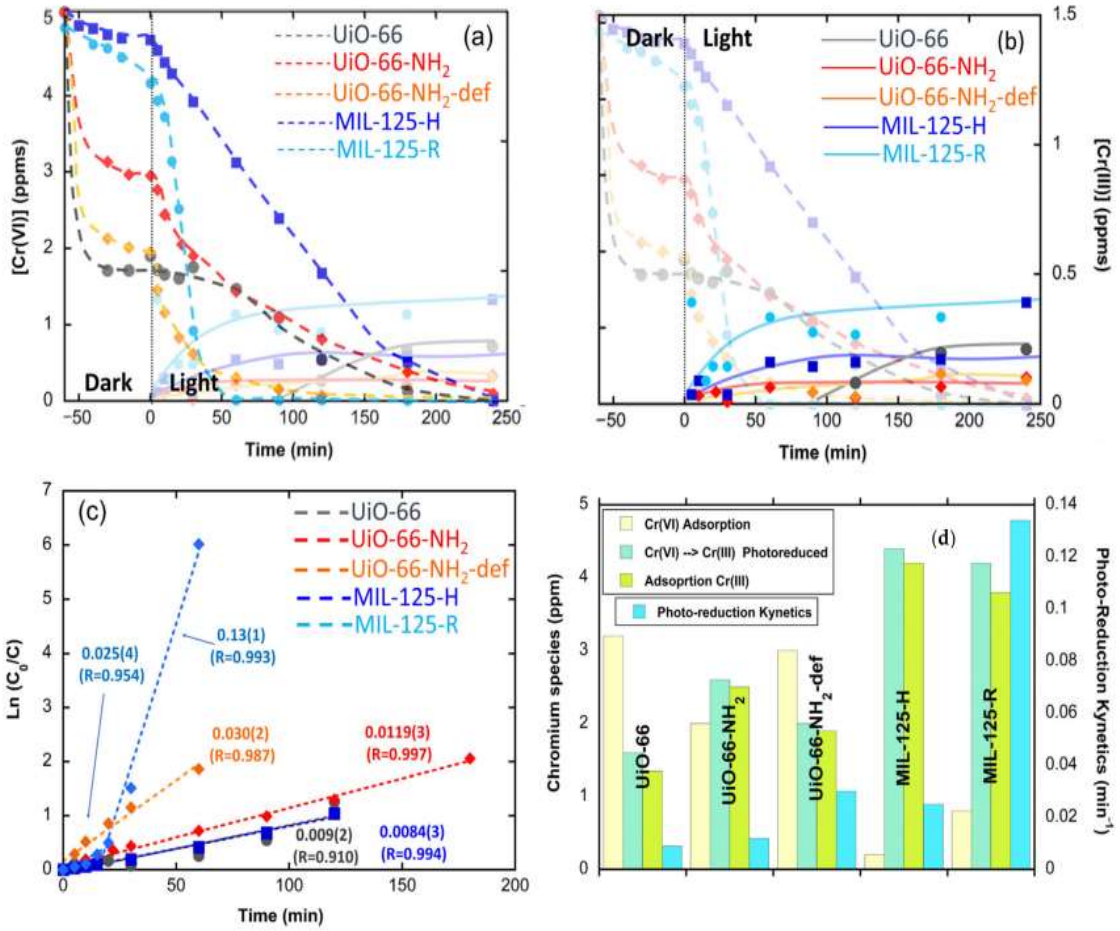

Figure 1 Potential energy profile for the CO2 hydrogenation pathway on ZrO2-modified Cu surfaces.

3.3 Selectivity and Product Distribution

Microkinetic simulations calculated the product distribution at 50 bar pressure. The model shows that methanol selectivity stays above 75% in the temperature range of 500–540 K. Fig. 2 displays the effect of temperature on the CO_2 conversion and methanol yield. As shown in the figure, higher temperatures favor the reverse water-gas shift reaction, which produces CO. However, the ZrO_2-modified surface suppresses this side reaction. This suppression happens because the interface sites bind oxygen strongly. This strong binding makes the breaking of the C–O bond difficult. This behavior differs from pure copper, where CO is often the main product [16].

ISSN: 3079-9341

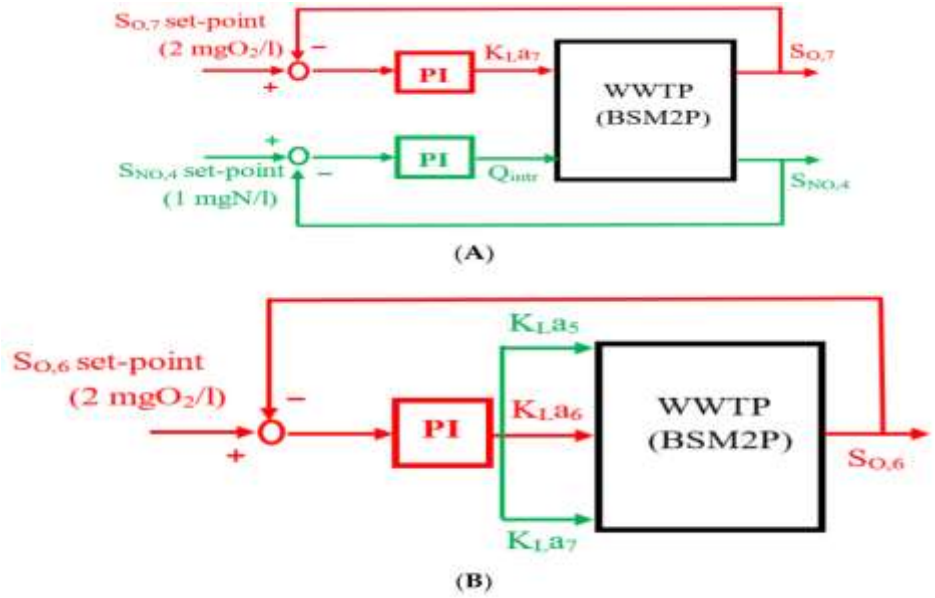

Figure 2 Effect of temperature and pressure on the equilibrium conversion of CO2 and methanol yield.

3.4 Role of the Interface in Network Reshaping

Comparing the formate and CO pathways shows a shift in the reaction network. On pure copper, the surface binds intermediates weakly. This weak binding causes a high barrier for hydrogenation and favors CO release. In contrast, the ZrO_2–Cu interface acts as a bifunctional site. The zirconium oxide activates the oxygen atoms of CO_2, while the copper activates the hydrogen. This combined effect changes the energy landscape. It opens a low-energy channel for formate hydrogenation that bypasses the difficult CO formation step. This network change explains the high methanol production seen in experiments [17].

4.Conclusions

In this paper, a reaction network with 41 elementary steps was constructed to study CO_2 hydrogenation on ZrO_2-modified Cu surfaces. The results show that the interface reduces the energetic span of the formate pathway to 0.69 eV. This value is much lower than that on pure copper. The analysis identifies the hydrogenation of bidentate formate as the rate-determining step. The interface stabilizes this transition state. This stabilization explains the high methanol selectivity of over 75% found in the simulations. These findings prove that the oxide-metal boundary changes the reaction network to favor methanol. This work helps in the optimization of inverse catalysts. However, the current models are ideal and periodic. Future research should consider real nanoparticle shapes and defects to improve accuracy.

ISSN: 3079-9341

References

[1] Sen, R., Goeppert, A., & Surya Prakash, G. K. (2022). Homogeneous hydrogenation of CO2 and CO to methanol: the renaissance of low-temperature catalysis in the context of the methanol economy. Angewandte Chemie International Edition, 61(42), e202207278.

[2] Peng, H., Dong, N., Liao, Y., Tang, Y., & Hu, X. (2024). Real-Time Turbidity Monitoring Using Machine Learning and Environmental Parameter Integration for Scalable Water Quality Management. Journal of Theory and Practice in Engineering and Technology, 1(4), 29-36.

[3] Sajnani, S., Memon, M. A., Memon, S. A., Kumar, A., Mehvish, D., Ameen, S., ... & Liu, Y. (2025). CO2 to Methanol Conversion: A Bibliometric Analysis with Insights into Reaction Mechanisms, and Recent Advances in Catalytic Conversion. Processes, 13(2), 314.

[4] Xu, K., Xu, X., Wu, H., & Sun, R. (2024). Venturi Aeration Systems Design and Performance Evaluation in High Density Aquaculture.

[5] Leybo, D., Etim, U. J., Monai, M., Bare, S. R., Zhong, Z., & Vogt, C. (2024). Metal–support interactions in metal oxide-supported atomic, cluster, and nanoparticle catalysis. Chemical Society Reviews.

[6] Yang, Z., Kumari, S., Alexandrova, A. N., & Sautet, P. (2025). Catalytic Activity of an Ensemble of Sites for CO2 Hydrogenation to Methanol on a ZrO2-on-Cu Inverse Catalyst. Journal of the American Chemical Society, 147(18), 15294-15306.

[7] Onishi, N., & Himeda, Y. (2024). Toward methanol production by CO2 hydrogenation beyond formic acid formation. Accounts of Chemical Research, 57(19), 2816-2825.

[8] Xu, K., Xu, X., Wu, H., Sun, R., & Hong, Y. (2023). Ozonation and Filtration System for Sustainable Treatment of Aquaculture Wastewater in Taizhou City. Innovations in Applied Engineering and Technology, 1-7.

[9] Pérez-Botella, E., Valencia, S., & Rey, F. (2022). Zeolites in adsorption processes: State of the art and future prospects. Chemical reviews, 122(24), 17647-17695.

[10] Wang, Y., Wang, Y., Yin, X., Arias, R., & Chen, J. (2026). Research on Dynamic Assessment of Glucose-Lipid Metabolism and Personalized Drug Response Prediction Based on Wearable Multimodal Sensing.

[11] Bac, S., & Mallikarjun Sharada, S. (2022). CO oxidation with atomically dispersed catalysts: insights from the energetic span model. ACS Catalysis, 12(3), 2064-2076.

[12] Weber, J. M., & Lapkin, A. A. (2023). Micro-kinetics analysis based on partial reaction networks to compare catalysts performances for methane dry reforming reaction. Chemical Engineering Journal, 466, 143212.

[13] Wang, C., & Chakrapani, V. (2023). Photocatalytic generation of reactive oxygen species on Fe and Mn oxide minerals: mechanistic pathways and influence of semiconducting properties. The Journal of Physical Chemistry C, 127(48), 23189-23198.

ISSN: 3079-9341

[14] Kistler, T. A., Prabhakar, R. R., & Agbo, P. (2024). A recirculation system for concentrating CO 2 electrolyzer products. Sustainable Energy & Fuels, 8(10), 2292-2298.

[15] Wang, C., & Chakrapani, V. (2023). Environmental Factors Controlling the Electronic Properties and Oxidative Activities of Birnessite Minerals. ACS Earth and Space Chemistry, 7(4), 774-787.

[16] Korányi, T. I., Németh, M., Beck, A., & Horváth, A. (2022). Recent advances in methane pyrolysis: turquoise hydrogen with solid carbon production. Energies, 15(17), 6342.

[17] Cannizzaro, F., Hensen, E. J., & Filot, I. A. (2023). The promoting role of Ni on In2O3 for CO2 hydrogenation to methanol. ACS catalysis, 13(3), 1875-1892.